

# Supporting Tool for Clinical Observation of the Eyeballs Movements

Agata Jurkowlaniec, Michał Szulc, Tomasz Dybizbański, Sławomir Michalak,  
Aleksandra Świetlicka, Karol Gugąła, and Andrzej Rybarczyk

**Abstract**—The tool was created to support the auxiliary clinical observation of the eyeballs movements in cases of different states of consciousness. It enables performing objective observation of the patient reaction to a given external light stimuli. The tool analyzes the coordination of the eyeballs movement with the position of the light stimuli. Images are obtained by camera equipped with infrared filters blocking all visible light with the cutoff light length 715nm.

**Keywords**—image processing, eyeball movements tracking, cranio-cerebral injury.

## I. INTRODUCTION

THE consequence of a global cerebral ischemia or a cranio-cerebral injury are chronic consciousness disorders. They lead to the secondary pathology in the central nervous system [1].

Different chronic consciousness disorders were observed in a group of patients and they were specified as minimal consciousness state, akinetic mutism, locked-in syndrome and persistent vegetative state. Different signs and symptoms are characteristic for each of these syndromes.

The minimal consciousness state [2] is diagnosed in cases able to perform voluntary movements like grasping or reaction to sounds or visual tracking of moving objects. The akinetic mutism patient does not responds to verbal stimuli (mutism), nor does not perform any spontaneous movements (akinetic). The locked-in syndrome is characterized by maintained consciousness that differentiates this condition from akinetic mutism. The patient is unable to perform any spontaneous movement with exception of eyeballs and eyelids movements. Basing on such movements the patient can communicate with other persons.

In vegetative state the simple reactions of the patient can result from brain stem activity. However the subject is unconscious. During persistent vegetative state the person is not perceptive [3]. That condition offers a very small chance for recovery. Coma is a condition in which there is no response to any stimuli, no spontaneous physical activity or contact with the environment.

Transition from one state to another [4] is possible and it can indicate clinical improvement and favorable outcome.

A. Jurkowlaniec, T. Dybizbański, M. Szulc, A. Świetlicka, K. Gugąła, and A. Rybarczyk are with Poznań University of Technology, Department of Computer Engineering, 60-965 Poznań, ul. Pitrowo 3A, Poland (e-mails: agata.jurkowlaniec@gmail.com; tomzyb@wp.pl; {michal.szulc; aleksandra.swietlicka; karol.gugala; andrzej.rybarczyk}@put.poznan.pl).

S. Michalak is with Department of Neurochemistry and Neuropathology, Chair of Neurology, Poznań University of Medical Sciences, Neuroimmunological Unit Polish Academy of Sciences (e-mail: slamic@yahoo.com).

The example of such situation is transition from locked-in syndrome to minimal consciousness state.

Therefore, the consciousness level evaluation is extremely important from the clinical point of view. It allows to take a decision regarding the patient's treatment and further procedures and furthermore it defines the prognosis. Clinical evaluation of the observed response and the reactivity level to external stimuli can be biased by the examiner's subjective interpretation. The use of supporting tool during observation of spontaneous eyeball movement and tracking of objects moving in the environment could be very helpful and improves the objectivity of the observations.

The examination of patients after cranio-cerebral trauma performed by a doctor is based on observation of patients' reaction to a given stimulus. The tracking of horizontally moving object, which is usually a low-power light source such as weak light bulb placed at the end of the pen, is observed.

Conscious patient can control voluntary eyeball movements and will try to track an object. However, consciousness disturbances cause limitations in such a reaction. The clinical evaluation can be challenging in certain cases. Such a testing is also limited by subjective examination, which may lead to incorrect assessment of impaired consciousness, and thus determine improper evaluation. Clinical conclusion considered by different examiners can be contradictory.

The paper describes the tool that helps perform objective clinical evaluation. The basis for its action is to record data on the patient's eyeball movements, which are the result of a light stimulus controlled by the computer software. Recorded data include information about the point in space, where, at any given time, the patient focuses the gaze and the location of the light stimulus at the same time. The results of the study are presented as a graph in time.

## II. THE TOOL OVERVIEW

### A. The Concept of Tool

The tool is equipped with a digital camera which provides the images of the patients eyes. Analysis of the images gives the information of the patients eyeball moments being the reaction to a given precise light impulses (stimulus). Part of the tool is a computer which controls the parameters of the emitted light impulses. Examined patient is in the bed in a half seated position, with gaze fixed on the device generating the light stimulus points – see Fig. 1. It is placed in front of the tested patient at the level of his eyes in a distance between 1,5 to 3 meters. The device used to emit the light impulses points is called LED light line (LED LL).

The images from camera are analyzed and based on the obtain information's the Probable Point of Gaze Focus (PPGF) is calculated. The time-correlated data from the LED LL (instantaneous position of the light impulse) and PPGF calculations are presented graphically on the computer screen to the examiner. The image analyzing program is able to include in the PPGF calculations the small head movements of the examined patient.

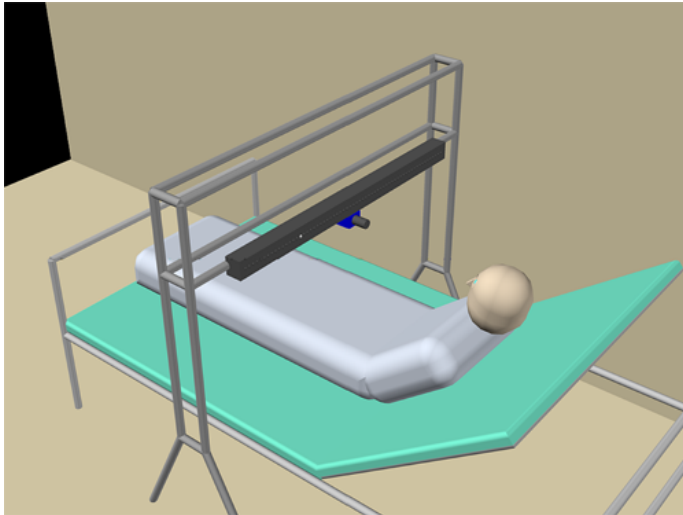


Fig. 1. Visualization of the patients position during the examination, the LED LL device and the camera.

### B. The Tool Design

The LED LL is light impulses (stimulus) generating device. The stimulus is created by the sequence of light pulses with specific time characteristics. The device is a modular design built of eight identical segments each using the FLUX type LEDs evenly distributed over. The FLUX type LEDs are characterized by the luminous intensity range 1000-3000 mCd, no focusing lenses and wide angle lightning. These properties are extremely important in order to maintain the uniform and independent of the angle of view light stimuli.

The LED LL is controlled by the microprocessor based system communicating with the PC class system. The communication enables close cooperation between the control software ran on the computer and their mutual synchronization. The precise timing of the light impulses generated by the LED LL (location and time of onset of the light pulse) and the image acquisition process are crucial for the proper system functioning.

Each segment of the LED LL includes eight LEDs. The communication between the segments occurs through the  $I^2C$  bus, while the RS-232 standard is used in communication between the LED LL and the PC class computer.

### C. Camera

The tool is equipped with the digital CCD camera with a FireWire port. Its capable of recording images at 30 frames per second. The camera is equipped with zoom lens of 5 to 50

mm focal lengths. It has been rebuilt to enable a near infrared operation. Camera is equipped with low-pass infrared filters with cutoff wavelength 715nm.

Recording images using the camera modified as above allows to obtain stable and light color temperature independent acquisition of pictures. Images are free from light reflections and glare – see Fig. 2. The analysis of acquired eye image in the near-infrared spectrum is less complex than the one acquired in visible range of light [5], [6]. The camera mounting is designed in the way to allow the precise adjustment of the optical axis in vertical plane in order to acquire the precise image of the eyes of the tested patient.



Fig. 2. Example images of the same eye done with the non-modified camera done in the visible range of light (left) and done with the same modified camera in near-infrared spectrum (cutoff light length 715nm) (right).

### D. Control Software

The OpenCV and Qt libraries are multiplatforms libraries and therefore the software is portable and currently available for MS Windows and Linux operating systems. The tool is controlled by the software run on a computer. The image analysis procedure uses the OpenCV library (available under a BSD license) and the implemented user interface is based on Qt library (available under LGPL license). Because both libraries used in the project are multi-platforms libraries therefore The OpenCV and Qt libraries are multiplatforms libraries and therefore the software is portable and currently available for MS Windows and Linux operating systems.

## III. PROCEDURE OF CALCULATING THE PPGF

### A. Theoretical Basics

The main task of the tool is to determine the point (PPGF) on the LED LL at which the patient is focusing gaze. The PPGF calculations are based on the following anatomical and physiological properties of the eye. Adults eyeball is approximately a sphere with a diameter of 24 mm. The eyeball of the adult person is approximately 24 mm wide in diameter. The iris has a diameter of about 12 mm, and the pupil has a diameter between 3 to 8mm. The eyeball is located in the orbital cavity and the only possible movement is rotation. The center of the rotation is situated in the center of the eyeball which is 12 mm behind the cornea on the eyeball optic axis [7].

The Figure 3 shows the representation of the eyeballs and LED LL in a two-dimensional coordinate system. The PPGF on the LED LL is calculated based on the previously determined optic axes. Each of the axes (for the left and the right eye) is determined from a hypothetical straight line passing through the center of pupil and the rotation point. The center of the eyeball is estimated from the distance between the

eyeballs and plane of the LED LL measured at the beginning of the examination process.

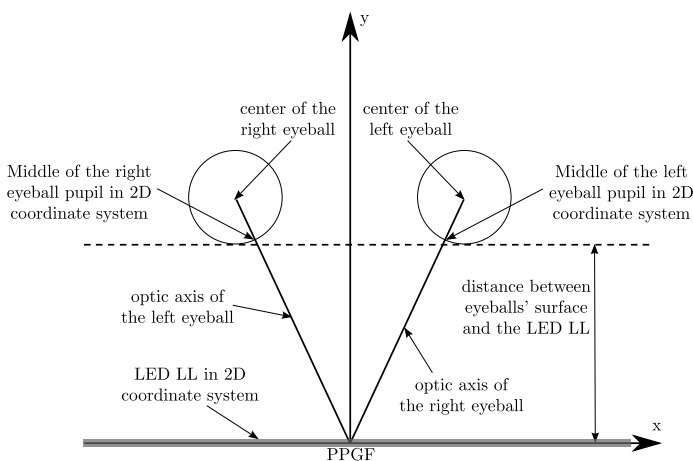


Fig. 3. Representation of the eyeballs and LED LL in a two-dimensional coordinate system.

There are many known gaze tracking methods [8], [6], [9]. Most of them are based on tracking and localization of the corneal reflex. Those methods require high quality high resolution images. The tests conducted on selected implementation of the known methods have shown that the calculations of the pupil localization are insufficiently precise. This work proposes a method based on the accurate pupil localization on the low resolution images.

The calculations of the center of the pupil are based on the camera image. In the presented method the camera should be positioned so that the image contains symmetrically placed pictures of eyes. During the examination the patients eyes cannot be closed.

The efficient implementation of the method allows for real-time pupil localization and real-time PPGF calculations.

### B. The Proposed Method of the Pupil's Center Localization and Computation of the PPGF

Various methods for the iris localization and the segmentation problem have been proposed [10], [11]. In this work we present custom-designed, highly problem-specific and computationally efficient method. The proposed method allows for the real-time computation of the pupil's center localization for both eyes when run on a 1.86 GHz single core PC class system.

The proposed method of localization of the pupil center and the computation of the PPGF is based on the following algorithm, the main stages of which are presented below:

- 1) Load image frame from the camera
- 2) Convert to gray image
- 3) Find inner area (an inner rectangle) containing the pupil image – threshold the image (outer rectangle) with the threshold value based on image luminosity. It should be noted that the above procedure is being used independently for each eye
- 4) Reduce the image noise with median filter

- 5) Compute the  $O$  point – the geometric center of the thresholded image
- 6) Compute the ROI (Region of Interest) being the square with the center in  $O$  and size determined by the human-assisted calibration procedure executed at the beginning of the examination procedure. Further processing is done only inside of the ROI of the gray image
- 7) Find the center of the pupil within the computed ROI according to the procedure presented in details in section C below.
- 8) Compute slight head movements of the examined patient based on the marker situated above the eyes
- 9) Update the coordinates of the pupil center in two-dimensional coordinate system using in the calculations: center of the pupil (step 7) and the values of the head movement (step 8).
- 10) Compute the final coordinates of the PPGF on the LED LL.

Results of the processing done in steps 1, 2, 3 and 8 are presented in Fig 5.

### C. Algorithm Used to Localize the Center of the Pupil

The following, custom-designed algorithm is used to calculate the coordinates of the center of the pupil within the ROI of the gray image determined in step 6. of the algorithm from section B.

```

while( (number_of_iterations < 10) and (PPGF_found==false) )
inner_image_orig = find_inner_area_containing_the_pupil_image()
threshold = threshold_init_value
inner_image = threshold(inner_image_orig, threshold)
contours[] = Find_contours_for_black_coloured_object()
c_size = contours[].size
good_contours[] = NULL

for (i=1..size, j=1)
if ((contours[i].length>min_contour_length)
    and(contours[i].length<max_contour_length))
    good_contours[j] = contours[i]
if (good_contours[j].size == 0)
    threshold = adapt_threshold( threshold, contours[] )
    break
else
    good_circles[] = NULL
    gc_size = good_contours[j].size
    too_big_circle_found = false

for (i=1..gc_size, j=0)
temp_circle = circumscribe_circle( good_contours[i] )
if (temp_circle.radius < max_circle_radius)
    good_circles[j] = temp_circle
else
    too_big_circle_found = true
    break
if (too_big_circle_found = true)
    threshold = adapt_threshold( threshold, circles[] )
    break
else
    if( good_circles[j].size = 1 )
        best_circle = good_circle[1]
    else
        for (i=1..good_circles[j].size , j=0)
            if ( i == 1 )
                best_features = comp_features(good_circles[i])
                best_circle = good_circles[i]
            else
                curr_features = comp_features(good_circles[i])
                if ( is_curr_features_better(curr_features,best_features) )
                    best_features = curr_features
                    best_circle = good_circles[i]
return best_circle

```

Fig. 4. Procedure for finding the center of the pupil.

Results of the subsequent processing steps are presented in Figures 6, 7 and 8. Here below is a more detailed description of the functions used in algorithm presented in Fig. 4.

**find\_inner\_area\_containing\_the\_pupil\_image()** – threshold the image (outer rectangle) with the threshold value based on image luminosity then compute  $O$  – the geometric center of the binarized image and finally compute the ROI being the square with the center in  $O$  and size determined by the human-assisted calibration procedure.

**find\_contours\_for\_black\_colored\_object( inner\_image )** – finds contours of all the black colored objects in the thresholded inner image (i.e. the ROI computed in the **find\_inner\_area\_containing\_the\_pupil\_image** function).

**adapt\_threshold( threshold, contours[] )** – adapt the threshold value used by the **find\_contours\_for\_black\_colored\_object** function. Adaptation algorithm is based on the current threshold value and the analysis of the lengths of the contours.

**adapt\_threshold( threshold, circles[] )** – adapt the threshold value used by the **find\_contours\_for\_black\_colored\_object** function. Adaptation algorithm is based on the current threshold value and the analysis of the parameters of the circumscribed circle.

**circumscribe\_circle( good\_contours[i] )** – finds the points belonging to the circle circumscribed on the contours found by the **find\_contours\_for\_black\_colored\_object** function.

**comp\_features( good\_circles[i] )** – compute the selected parameters of the circumscribed circle.

**is\_curr\_features\_better( curr\_features, best\_features )** – compare quality of the features of the currently found circumscribed circle with the features of the best found circumscribed circle.

#### D. Head Movement Correction

The preliminary tests of the method of pupil center localization and calculation of the PPGF have showed that during the examination person's head was moving slightly. Those movements were the result of the physiological actions like breathing or heart beating. The preliminary tests have also shown that disregarding the movements in PPGF calculations results in incorrect PPGF calculations. To solve the problems a method has been designed to enable the correction of the horizontal movements of the head. The method is based on the additional marker placed between the eyes. The marker is tracked and its position is being calculated simultaneously with the eyes tracking procedure. The position of the marker is then used to calculate the head movement correction parameter.

## IV. THE EXPERIMENTAL RESULTS

### A. Procedure Used to Localize the Pupil Center

The tool has been tested repeatedly on six healthy subjects. The following presents the selected results of the pupil localization procedure.

Figures 9 and 10 present images of the eyes with the localized pupil center for two individuals with different shapes of eyes and with different color of iris. The test has been carried out in daylight with no additional light sources.

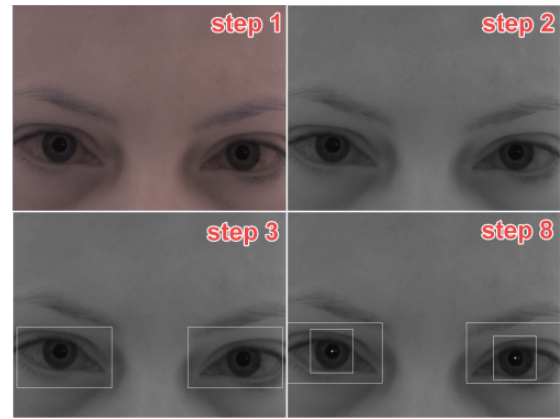


Fig. 5. Example images presenting results of selected steps of the algorithm from section III.B (steps: 1, 2, 3 and 8).

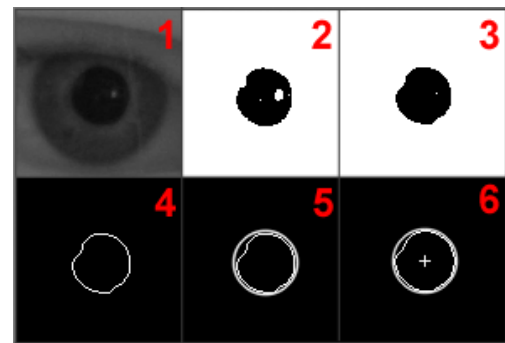


Fig. 6. Example of the correct pupil center localization (step 8) for the image of the eye directed forward. Examples of the analysis process.



Fig. 7. Example image of the eye in half-extreme position and the successful circumscribed circle on the one of the two contours found in the ROI with two black-coloured objects.

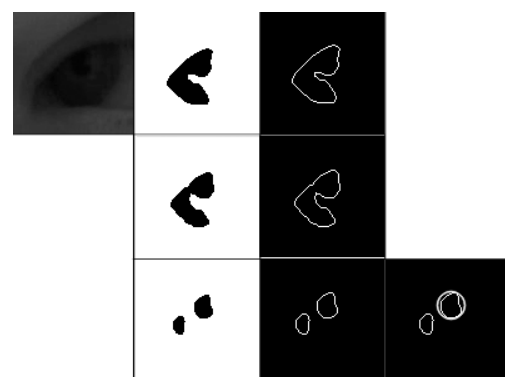


Fig. 8. An eye sample image in extreme position with partially hidden pupil and steps of analysis in order to find the contour of the pupil. The result is correct circumscribed circle on the one of the two contours found in the ROI with two black-coloured objects.

During the tests the following limitations of the procedure has been observed:

- 1) the successful pupil center localization is sensitive to the proper eye illumination that should be relatively strong and diffused. The strong, point light source in some particularly rare conditions can significantly disrupt the proper pupil center localization;
- 2) the procedure in some rare conditions can erroneously detect pupil center localization in the case of the iris image obstruction due to eyelashes;
- 3) the procedure cannot properly detect the closed eye image and in some rare cases it can erroneously detect the false pupil center localization.

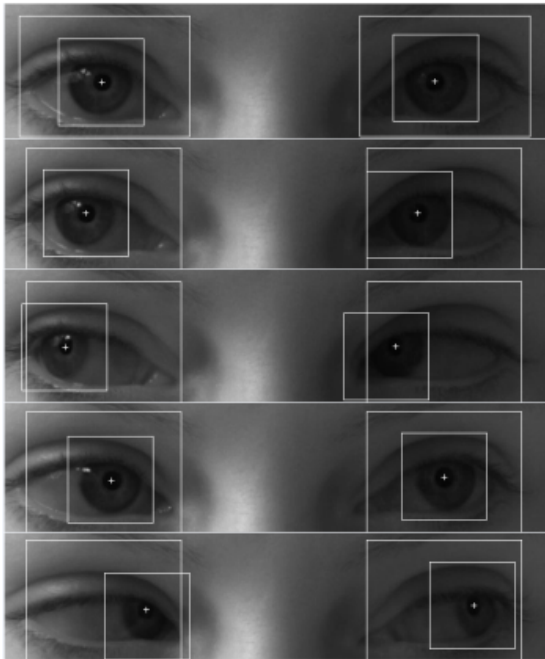


Fig. 9. Example of pupil center localization for person 1 (female, brown iris).

### B. Tracking the Light Stimulus

Diagrams with the results of the light stimulus tracking are presented below. A single diagram shows the position of the light stimulus and the position of the calculated PPGF. The ideal tracking results are presented on the diagram as two points – the calculated PPGF and the location of the light stimulus – having equal coordinates. This situation is impossible to attain in real-world experiments due to the some delay associated with the eye response time to the stimulus. In the real-world experiments it is assumed that the tracking is successful when those two points also close together and thus the time plots of the PPGF and light stimulus are similar in shape. The time plots with the results of the tracking procedure for two different individuals are presented in Fig. 11 and Fig. 12.

Figure 11 shows the effect of head movement correction. The examined person was correctly responding to the light stimuli. The time plots representing the PPGF calculations without correction are shifted compared to plots of the light stimuli positions.

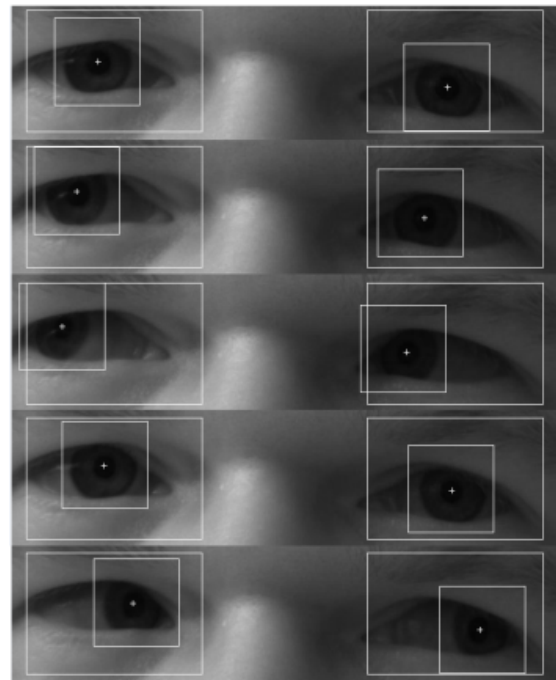


Fig. 10. Example of pupil center localization for person 2 (male, green iris).

The tests have shown that PPGF is calculated successfully in cases when the patient is looking at the light impuls on LL *not being* in the extreme left or right position. The extreme left and right positions of the light impuls on the LL often require from the patient the substantial head movement towards the light impuls. In this cases the head movement correction method is unable to compute the required adjustment, which increases the error in the PPGF calculation. Also in extreme left and right positions the pupil can be underexposed depending on the level of the lightening. The incorrectly calculated PPGF can be observed in Fig. 11 and Fig. 12.

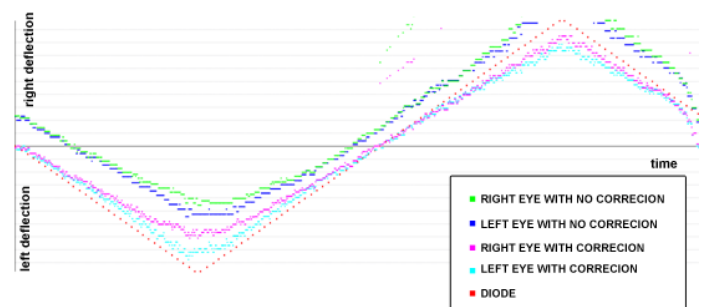


Fig. 11. The time plots of the light stimulus tracking for Person 1. The effects of the head movements corrections are visible.

## V. CONCLUSION

The tool was created to assist the observation of response to a given light stimuli of patients with different consciousness disorders. Only the healthy persons was tested (members of the design team). Testing real patients requires the permission of the bioethical commission which is not given yet.

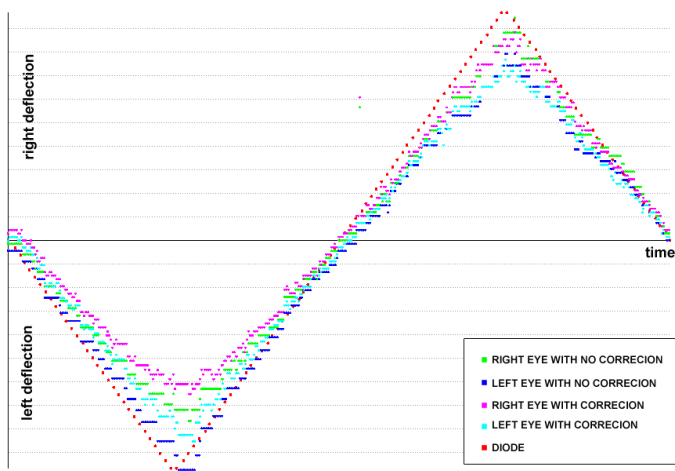


Fig. 12. The time plots of the stimulus tracking for Person 2.

The examination of the tool brought a conclusion that it can be used in cases of patients not only with different consciousness disorders but with different neurological diseases. The example is myasthenia – the disease leading to rapid muscle weakness and fatiguability. The graphic representation of the data can be applied to show the delays in the increasing time of eye muscle reaction to the light stimuli and asymmetry of eyeballs movements. Another field of use is evaluation of syndromes in case of synchronicity, apokamnosis or strabismus. Further test performed with the tool will show the future possibilities of using it in different diseases and cases.

## REFERENCES

- [1] S. Michalak and J. Mejnartowicz, *Zespoły objawowe w neurologii*. Wydawnictwo Lekarskie PZWL, 2006, in Polish.
- [2] J. T. Giacino, S. Ashwal, N. Childs, R. Cranford, B. Jennett, D. I. Katz, J. P. Kelly, J. H. Rosenberg, J. Whyte, R. D. Zafonte, and N. D. Zasler, "The minimally conscious state. Definition and diagnostic criteria," *Neurology*, vol. 58, pp. 349–353, 2002.
- [3] D. D. Tresch, F. H. Sims, and E. H. Duthie, et al., "Clinical characteristics of patients in the persistent vegetative state," *Arch. Intern. Med.*, vol. 151, 1991.
- [4] N. L. Childs and W. N. Mercer, "Brief report: Late improvement in consciousness after post-traumatic vegetative state," *New England Journal of Medicine*, vol. 334, no. 1, pp. 24–25, 1996.
- [5] T. Nagamatsu, J. Kamahara, and N. Tanaka, "3D gaze tracking with easy calibration using stereo cameras for robot and human communication," *Robot and Human Interactive Communication*, pp. 59–64, 2008.
- [6] H. C. Lee, D. T. Luong, C. W. Cho, E. C. Lee, and K. R. Park, "Gaze tracking system at a distance for controlling IPTV," *Consumer Electronics, IEEE Transactions*, vol. 56, pp. 2577–2583, 2010.
- [7] A. Bochenek and M. Reicher, *Anatomia człowieka*. Warszawa: PWZL, 1965, vol. VII, in Polish.
- [8] D. H. Yoo, J. H. Kim, B. R. Lee, and M. J. Chung, "Non-contact eye gaze tracking system by mapping of corneal reflections," in *Automatic Face and Gesture Recognition. Proceedings of the Fifth IEEE International Conference*. IEEE Computer Society Washington, 2002, pp. 94–99.
- [9] X. Yang, J. Sun, J. Liu, J. Chu, W. Liu, and Y. Gao, "A gaze tracking scheme for eye-based intelligent control." *Intelligent Control and Automation (WCICA)*, 2010, pp. 50–55.
- [10] W. Sankowski, K. Grabowski, M. Napieralska, M. Zubert, and A. Napieralski, "A knowledge-based approach to the iris segmentation problem," *Image and Vision Computing*, vol. 28, pp. 238–245, 2010.
- [11] T. Tan, Z. He, and Z. Sun, "Segmentation of visible wavelength iris images captured At-a-distance and On-the-move," *Image and Vision Computing*, vol. 28, 2010.